Experimental results of environmental-based passive time reversal in underwater communications

Lussac P. Maia, António Silva, Sérgio M. Jesus

LARSyS, Campus de Gambelas, Universidade do Algarve

8005-139 Faro, Portugal

Email: lussacmaia@gmail.com, {asilva,sjesus}@ualg.pt

Abstract—This paper presents experimental results of coherent communications comparing the following methods of underwater channel identification applied to a time-reversal processor: pulse compression, L1-norm regularization and channel physical modeling. The first method is the Passive Time Reversal in its conventional form: a low complexity technique to mitigate inter-symbol interference due to multipath propagation; the second method is an estimator of sparse channels, inspired by the theory of compressed sensing; and the third method is the proposed environmental-based approach that generates channel replicas through inverse numerical modelling using the physical properties of the underwater media between the emitter and the receiver. Data from a quadrature-phase-shift-keyed low resolution image transmitted on May 27, 2011 during the Underwater Acoustic Network 2011 experiment conducted off the coast of Throndheim (Norway), are processed using these three methods and their mean square error performance is compared. The results show that the proposed environmental-based approach outperforms the other two channel identification methods by one to four dB over the duration of the transmitted image packet.

I. Introduction

Performing digital acoustic underwater communications at high data rate is a challenging problem, mainly due to the need to compensate for a double spreading channel and the requirement to use a coherent signaling scheme to increase the data throughput. The channel has double spreading because (i) multipath propagation causes spreading of path delays in the channel impulse response (CIR) generating inter-symbol interference, and (ii) frequency spreading causes both carrier offset and signal spectrum distortion. Compensating for such distortions of the underwater channel by applying a robust coherent equalizer is essential for high data rate message recover.

A well-known low complexity channel compensation method for underwater communications is the Passive Time Reversal (PTR), which mitigates inter-symbol interference by performing synthetic time signal retro-focusing, assuming that the receiving array sufficiently spans the water column for capturing the most significant propagating acoustic modes and the CIR estimates are sufficiently stable in time [1], [2]. PTR requires channel probing for obtaining CIR estimates to be used in their conjugate reverse filters, usually employing a pulse with suitable correlation properties to estimate the channel with Pulse Compression (PC). Another possible channel estimator is the Regularized ℓ1-Norm (RegL1), designed to identify sparse channels and widely employed in compressive

sensing theory [3], [4]. RegL1 yields cleaner CIR estimates then PC because of its higher immunity to noise and path side lobes effects, however it tends to suppress less significant paths. A different possibility for CIR estimate is to use an acoustic propagation model. However, since obtaining accurate CIR for communication channel compensation through simple direct modeling is difficult, acoustic inversion can be employed to generate appropriate CIR. Existing equalizers do not employ physical models in their design, lacking to incorporate the knowledge of acoustic propagation influent physical parameters into the communication channel replicas.

This work proposes a method for underwater channel compensation that explores the influence of acoustic propagation environmental parameters by jointly achieving acoustic inversion and PTR and is therefore termed as Environmental Passive Time Reversal or EPTR. The approach is to identify channel physical parameters by optimizing an objective function that correlates channel probe data with modeled replicas generated with a suitable numerical model constrained in a search space of a priori parameters. Then, refined CIR estimates corresponding to a posteriori parameters are selected and tested through a maximum output power criterion yielding the CIR to be time-reversed in PTR. The methodology is inspired in model-based techniques such as Matched Field Processing (MFP) for source localization [19] and Matched-Field Inversion (MFI) for the estimation of environmental parameters [12]. There is a large body of research in this field, much of which can be found in overview papers [14], [20]. Most of this effort was directed to low-frequency applications (say below 2 kHz) due to requirements of propagation range, bottom penetration or other. Applications above that frequency range are rare, possibly due to the modelling detail required for parameter estimation in the high-frequency (tens of kHz) regime. In our case we are not interested in physical parameter estimation, but solely in CIR modelling. The physical models Bellhop and Bounce [15] were used as forward acousti propagation models for generating CIR candidate replicas search space. Advantages of EPTR over the conventional PTR are to achieve noiseless CIR estimates and perform channel compensation together with physical parameters assessment. A disadvantage is to expend more computational cost. Furthermore, since PTR is limited to coarsely mitigate inter-symbol interference in nearly static channels [16], [17], time compression/dilation compensation pre-processing and phase

locking post-processing for phase rotation compensation are done together with EPTR.

Experimental results were achieved with EPTR applying the mean CIR modeled from acoustic inversion in time-reversal filtering. During the Underwater Acoustic Network 2011 (UAN11) experiment that took place in the Strindfjorden (Norway) in May 2001, a quadrature-phase-shift-keyed modulated image message transmitted at 4000 bits per second was received on a vertical line array of 16 hydrophones, 890 meters away and processed with the three algorithms: PC, RegL1 and EPTR. The results show that the EPTR outperformed the other two algorithms over a the whole time frame.

This paper is organized as follows: Section II presents the EPTR data model and shortly review the PC and RegL1 methods in PTR. Section III shows results of EPTR applied to real data from the Underwater Acoustics Network 2011 (UAN11) sea trial, and compares its performance to the conventional PTR performance. Section IV concludes the paper and indicates future work.

II. DATA MODEL

Consider that a low resolution image is to be transmitted through the underwater channel and received on a vertical array. The image pixels are ordinarily converted into a bit stream $a[n]$ that is digitally modulated with the Quadrature Phase Shift Key (QPSK) scheme. After appropriately up-sampled and heterodyne to the carrier frequency, the passband signal $\tilde{s}(t)$ is generated for transmission, being represented by

$$\tilde{s}(t) = Re\left[a[l]p(t - lT_s)e^{j2\pi F_c t}\right] \tag{1}$$

where

$$a[l] = e^{j2\pi(m[l]-1)/M}; \quad m[l] \in [1, ..., M] \tag{2}$$

The symbol interval is denoted by T_s, Re denotes real part, the symbol map size is M ($M = 4$ in QPSK), $p(t)$ denotes a pulse shape and F_c is the carrier frequency.

The time-variant CIR of the underwater waveguide for a particular receiver sensor can be represented digitally by a two-dimensional complex baseband variable $h[n, k]$, where k is the reduced-time delay for each propagating path of a CIR snapshot, which evolves along true time n. Note that each CIR snapshot represents a state of the time-variant channel where the degree of variability depends on a variety of factors, for example source-receiver relative movement and/or water column and sea surface variability. As discussed below the channel identification algorithms proposed and tested in this paper have different degree of adaptivity to cope with time-variant channels [24]. Assuming hereafter complex baseband equivalent representation, a noisy received signal $y[n]$ is

$$y[n] = \sum_k h[n, k]s[n - k] + w[n], \tag{3}$$

where $w[n]$ denotes additive random noise. Using matrix notation and assuming that $\mathbf{s} \in \mathbb{C}^{Q \times 1}$, $\mathbf{H} \in \mathbb{C}^{P \times R}$, $\mathbf{g} \in \mathbb{C}^{R \times 1}$

with $\mathbf{H}^T = [\mathbf{g}_1, \mathbf{g}_2, ..., \mathbf{g}_P]$, where $\mathbf{g}_p$ is the p-th snapshot and $P = Q + R - 1$ allows to rewrite (3) as

$$\mathbf{y} = diag(\mathbf{S}\mathbf{H}^T) + \mathbf{w}, \tag{4}$$

where matrix $\mathbf{S}$ has Toeplitz structure, being computed from zero-padded $\mathbf{s}$ with $\mathbf{S} \in \mathbb{C}^{P \times R}$.

Further, one may observe that the system can be assumed as linear time-invariant whether frequency offset due to transmitter-receiver impairments or any Doppler trend due to sensors motion is compensated and under the assumption that any other channel variability effects are negligible. Thus, since the snapshots are assumed time-invariant, the received signal becomes

$$y[n] = \sum_k g[k]s[n - k] + w[n] = s[n] * g[k] + w[n] \tag{5}$$

where $g[k] \simeq h[0, k]$ if assumed a initial snapshot, or still $g[k] \simeq \bar{h}[n, k]$ if assumed an average snapshot (which is used in this work), and the symbol $*$ denotes convolution.

A. Passive time reversal

The PTR performs filtering of the received signal at each sensor of the array based on cross-correlation between the estimated (or modeled) CIR and the actual CIR. Mixing the filtered signals yields the PTR output as follows

$$z[n] = \sum_l z_l[n] = \sum_k Q[n]I[n - k] \tag{6}$$

with

$$I[n] = \sum_k s[k]R[n - k]; \quad R[n] = \sum_k p^*[k]p[n - k] \tag{7}$$

and thus

$$Q[n] = \sum_l \sum_k \hat{g}_l^*[k]g_l[n - k] \tag{8}$$

The R-function is the autocorrelation of the shaping pulse and the I-function is defined by the convolution of the R-function and the transmitted signal. The Q-function represents the cross-correlation between the estimated and actual CIR. The Q-function is particularly useful as an indicator of the PTR performance, since an impulse-like shape generally means a successful compensation of the multipath distortion. The present work processes real data, which precludes to know the actual CIR. However, an equivalent criterion for measuring the PTR performance is the PTR output average power at an observation interval of size N, given by

$$z_P = \frac{1}{N} \sum_{n=0}^{N-1} |z[n]|^2 \tag{9}$$

B. Channel identification

PTR processing requires channel identification information which is performed in this work by the PC, the RegL1 and model-based high-frequency acoustic inversion. The PC is a classical ℓ2-norm estimator which is robust and valid for general channel identification and the RegL1 includes a

weighted ℓ1-norm to solve a convex optimization problem in the particular case where the channel can be assumed as sparse [4]. One should observe that this may be often the case of shallow water underwater channels. A short description of these methods is presented below.

1) Snapshot CIR identification with classical ℓ2-norm estimator: The PC can be derived from the Minimum Variance Unbiased (MVU) estimator. Assuming a linear time-variant system $\mathbf{y} = \mathbf{Sg} + \mathbf{w}$ with $\mathbf{y}_l \in \mathbb{C}^{P \times 1}$, $\mathbf{g}_l \in \mathbb{C}^{R \times 1}$, $\mathbf{w}_l \in \mathbb{C}^{P \times 1}$ and $\mathbf{S} \in \mathbb{C}^{P \times R}$, the MVU estimator is

$$\hat{\mathbf{g}} = (\mathbf{S}^H \mathbf{S})^{-1} \mathbf{S}^H \mathbf{y}; \quad \mathbf{C}_{\hat{\mathbf{g}}} = \sigma_w^2 (\mathbf{S}^H \mathbf{S})^{-1} \quad (10)$$

where $\mathbf{C}$ denotes the estimator covariance. Note that the autocorrelation and cross-correlation properties of probe signal $\mathbf{s}$ directly affect the estimator performance, being a good choice to use a probe that makes the inverted matrix in (10) to appear close to diagonal. For the l-th hydrophone, the PC performs a cross-correlation based solution given by

$$\hat{\mathbf{g}}_l = \mathbf{S}^H \mathbf{y}_l \quad (11)$$

2) Snapshot CIR identification with regularized ℓ1-norm: The RegL1 is usually employed in compressive sensing for system identification in sparse channels, *i.e.* where the impulse response is characterized by a few strong arrivals at specific time delays and by nearly null magnitude for other delays. The optimization problem is defined as

$$P_l : \arg\min_{\mathbf{g}_l} \|\mathbf{g}_l\|_1 \quad \text{s.t.} \quad \mathbf{y}_l - \mathbf{Sg}_l \le \epsilon_{\mathbf{w}_l} \quad (12)$$

where $\epsilon_{\mathbf{w}}$ denotes a noise-driven error threshold. Unfortunately, there is no closed form solution for this problem. However, the problem can be solved with numerical computation by an iterative algorithm as, *e.g.* Least Absolute Shrinkage and Selection Operator (LASSO) or Least Angle Regression (LARS). In this work, the CVX model [18] is employed to achieve RegL1.

3) Inversion of acoustic propagation parameters and CIR: Figure 1 shows a block diagram of the model-based acoustic inversion channel identification module. The underwater
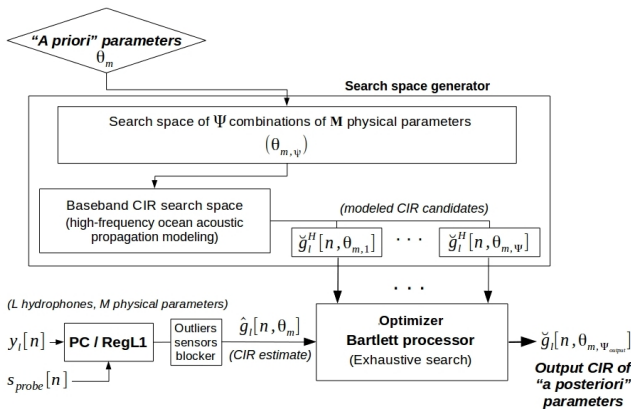

Fig. 1. Block diagram of the model-based acoustic inversion channel identification module for EPTR.

acoustic channel is parametrized by m physical parameters, so

that the corresponding CIR snapshot is written in explicit form as $g[n, \theta_n]$. Assuming that there is an a priori knowledge of the channel physical parameters, an appropriate search space of "a priori" parameters is created and the corresponding CIR candidate replicas generated through numerical modelling. The parameter search space in the present work contains the following physical parameters: source depth (SD), receiver depth (RD), source-receiver range (SRR), sediments compressional velocity (c_{p1}), sediments compressional attenuation (a_{p1}), sediments density (ρ_1). The other parameters required by the physical model have fixed values in order to limit the search space and therefore reduce the computational burden.

In the EPTR processor the CIR is first estimated with PC or RegL1 to generate the observed CIR, which is then used for the optimization to obtain the "a posteriori" noiseless modeled CIR candidates. The selection of such CIR candidates is done by maximizing a Bartlett objective function (Bartlett processor in Fig. 1) that compares observed data with the replicas built from a search space of a priori parameters, thus yielding the a posteriori physical parameters and the corresponding CIR.

The objective function used in EPTR for CIR snapshot modeling is defined in time-domain as

$$B(\psi) = \frac{\breve{g}_l^H[n, \theta_{m,\psi}] \left[\frac{1}{I} \sum_{i=1}^{I} \hat{g}_{l,i}[n, \theta_m] \hat{g}_{l,i}^H[n, \theta_m] \right] \breve{g}_{l,i}[n, \theta_{m,\psi}]}{\|\hat{g}_l[n, \theta_m]\| \|\breve{g}_l[n, \theta_{m,\psi}]\|} \quad (13)$$

where $\hat{g}$ denotes observed data and $\breve{g}$ denotes predicted data, such that $\hat{g}_{l,i}[n, \theta_m]$ means the CIR snapshot estimated from the i-th observation for the l-th sensor in the underwater environment parametrized by m acoustic propagation physical parameters. Similarly, $g_l[n, \theta_{m,\psi}]$, means the ψ-th modeled CIR snapshot (corresponding to the ψ-th set of m physical parameters contained in a search space of size Ψ) that is predicted for the l-th sensor. Note that using the maximum a posteriori criterion the best fitness candidate is reached by performing $B_{MAP} = \max_{\psi \in \Psi} B(\psi)$. The three CIR with best fitness are then processed with PTR to select the candidate that yields maximum output power, which is finally used in the time-reversal filtering. Further, since PTR is limited to coarse ISI mitigation, post-processing to compensate for phase rotation is performed.

A Maximum Power Decisor is employed to test the CIR candidates generated by the acoustic inversion algorithm and select the CIR that maximizes the PTR output power. The maximum power parameters set ψ_{mp} is given by

$$\psi_{mp} = \arg\max_{\psi_{output}} \frac{1}{N} \sum_{n=0}^{N-1} | \sum_l \breve{g}_l[n, \theta_{m,\psi_{output}}] * y_l^\dagger[-n] |^2 \quad (14)$$

where $*$ denotes convolution, $\dagger$ denotes conjugate and ψ_{output} denotes the few set of parameters obtained as output of the inversion. Thus, the output signal is

$$z_{mp}[n] = \sum_l \breve{g}_l[n, \theta_{m,\psi_{mp}}] * y_l^\dagger[-n] \quad (15)$$

III. EXPERIMENTAL RESULTS

Experimental results are presented for the data recorded on May 27, 2011, during the Underwater Acoustic Network 2011 (UAN'11) sea trial that took place in the Strindfjorden, Throndheim (Norway). Figure 2 shows the scenario with environmental information collected with dedicated equipment.
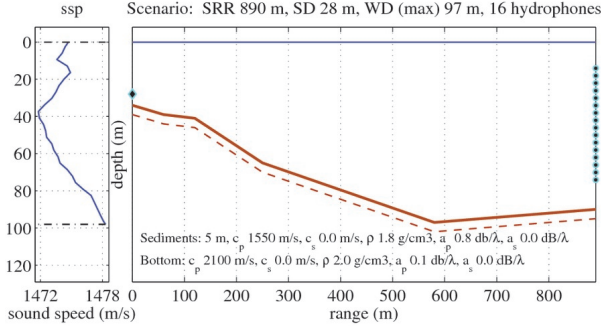

Fig. 2. Typical scenario of one transmit-receive leg of the UAN11 sea trial: sound speed profile taken on May 27, 2011 (left) and range-dependent transect ($890m$), source depth $28.1m$, 16 hydrophones vertical array $4m$ equally spaced from $14.1m$ to $74.1m$, maximum water depth $100m$, $5m$ sediments layer over bottom half-space (right).

The transmitted message is a stream of 71504 bits corresponding to the pixels of a low resolution gray image. This data is QPSK modulated so that 35752 symbols are generated to be the payload of a signal frame with fixed size of 50000 symbols. The frame structure is organized in order by a preamble m-sequence with 511 symbols, header with 40 symbols, payload and postamble m-sequence with 511 symbols. The preamble and postamble are used to perform time compression/dilation compensation, aiming at removing clock synchronization impairments between transmitter and receiver and a possible Doppler distortion, which is expected to be small since the sensors are moored. The payload contains a sequence of 20 short m-sequences with 127 symbols each, which are inserted every 1 second to track the channel variability and to be used in the acoustic inversion. The symbol sequence is upsampled and heterodyned to the carrier frequency of 25.6 kHz by the cNODE-Mini transponder model 34–180 provided by Kongsberg Maritime [21], which was specifically adapted for UAN'11 as decribed in [22]. The data is transmitted at a rate of 4000 bps to a vertical line array of 16 hydrophones positioned at 890 m along a range dependent transect with maximum 98 m water depth. The array spans from $14.1m$ to $74.1m$, $4m$ equally spaced.

A. Channel estimates and replicas from inversion

Figure 3 shows the wavefronts that reach the hydrophone array as estimated by PC (a), by RegL1 (b), modeled by high frequency acoustic inversion in EPTR based on PC (c) and modeled by high frequency acoustic inversion in EPTR based on RegL1 (d). One can clearly distinguish two main paths whereas the amplitude of the second arrival has a variable

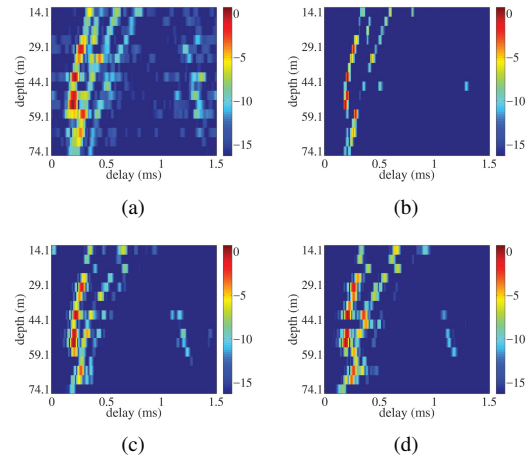amplitude along depth. The slight arrival angle of the main arrival may be due to an array tilt.

Fig. 3. Wavefronts estimated with PC (a), estimated with RegL1 (b) and modeled with high-frequency acoustic inversion by EPTR based on PC (c) and by EPTR based on RegL1 (d).

Figure 4 shows for channel 8 the time variability of the estimated CIRs again with PC (a), modeled with acoustic inversion based on PC (c), estimated with RegL1 (e) and modeled with acoustic inversion based on RegL1 (g). Also, the mean power of the CIRs is shown in the right column, (b), (d), (f) and (h) for the four cases, PC, modeled based on PC, RegL1 and modeled based on RegL1, respectively. Observe that the time-variant CIRs are sharper, *i.e.*, the path peaks have narrower lobes, when estimated with RegL1 than with PC. This is caused by the sparse estimator design that includes $\ell 1$-norm regularization to better explore the sparsity of the CIR in shallow water. Further, observe that, as expected, the modeled CIR generated by EPTR yields noiseless wavefronts and noiseless time-delay mean CIRs in comparison to PC, even though there are some delay mismatch for the later arrival.

The physical parameters that had the best match with the observed data are obtained as output of the acoustic inversion algorithm. Figure 5 shows, for snapshots 1 to 20, the evolution of the combination of geometrical physical parameters that generated the best CIR replica with EPTR based on PC. The geometric parameters are source-array range, source depth and hydrophone array depth, using the shallowest hydrophone as reference. Other physical parameters of the seabed were inverted (not shown), but aiming at improving the adjustment between replicas and observation, the so-called "focalization" as suggested in [12], [23]. The variability of the inverted "a posteriori" parameters observed in fig. 5 can be explained not only by the actual physical variability but also by the solution of an equivalent model that is influenced by the non-inverted parameters.

B. Communications performance

Figure 6 shows the results in terms of mean square error for the received signal after being processed by PTR with PC estimation (blue crosses), by PTR with RegL1 (red crosses),
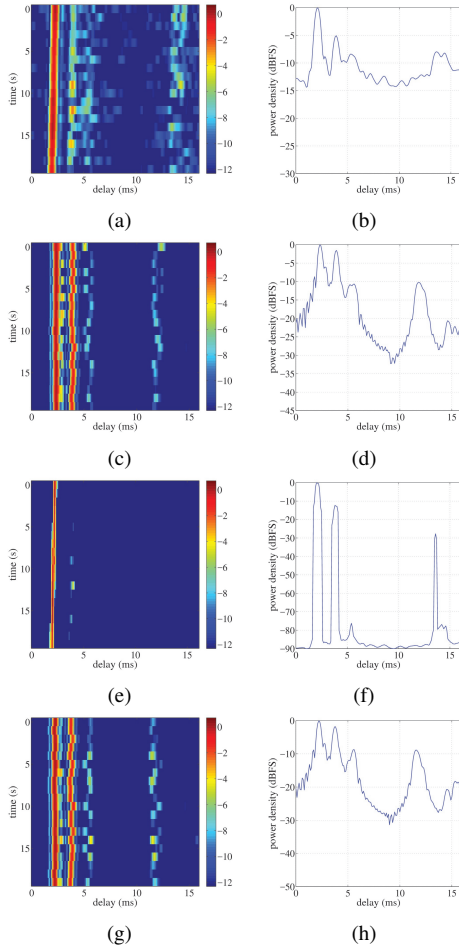
Fig. 4. Channel number 8 estimated CIR with PC (a,b), modeled with acoustic inversion by EPTR based on PC (c,d), estimated with RegL1 (e,f) and modeled with acoustic inversion by EPTR based on RegL1 (g,h). CIRs time variability (left) and mean power CIRs (right).
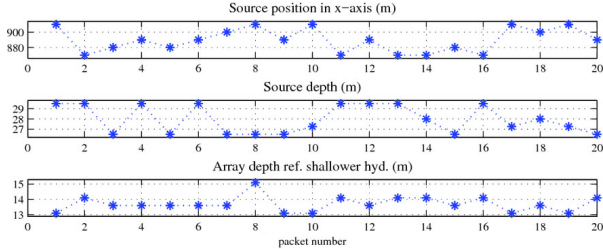

Fig. 5. "A posteriori" geometric parameters computed by the acoustic inversion algorithm for each of the 20 slots of the data frame using EPTR based on PC.

by EPTR with PC acoustic inversion (magenta circles) and by EPTR with RegL1 acoustic inversion (green stars), along 20 slots of signal frame containing the payload image data. The EPTR using acoustic inversion yielded the best results, with similar performance when using observed data from PC or RegL1. EPTR reached a performance significantly superior to PTR with PC estimation (that is used here as reference) and marginally better than RegL1. The improvement of EPTR
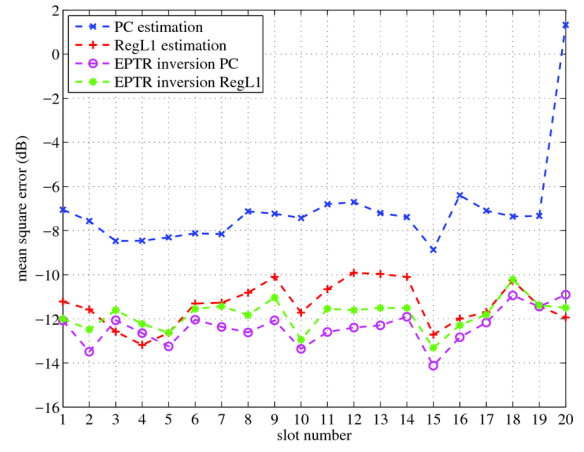

Fig. 6. Mean square error results with PC estimation (blue), RegL1 estimation (red), PC inversion (magenta) and RegL1 inversion (green).

inversion over PC estimation can be explained by the fact that the channel replicas obtained with inversion modeling are free of noise, which is an unavoidable drawback in the case of pulse compression. The EPTR based on PC has improved performance relative to EPTR based on RegL1. This is probably due to the fact that RegL1 tends to suppress less significant paths, which can probably degrades the matching between observation and modeled replicas performed by the acoustic inversion processor.

Figure 7 shows the received symbols along time after being processed by the conventional PTR (a) and with the EPTR based on PC (b). These constellations show that the cluster
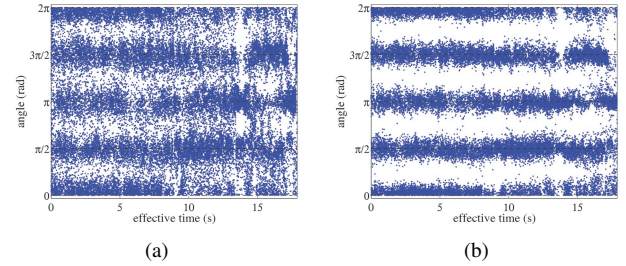

Fig. 7. Received symbols along time after processing with the conventional PTR (a) and with the EPTR based on PC (b). The vertical axis denotes the angles of recovered QPSK symbols. The horizontal axis is the effective time of payload transmission.

variance is clearly reduced in EPTR relative to conventional PC-based PTR.

Figure 8 shows the transmitted low resolution image (a), the recovered image with conventional PTR (b) and the recovered image after EPTR processing based on PC (c). The received image processed by the conventional PTR presents several wrong pixels. The image processed by EPTR (c) corrects most of such errors, yielding an image quite similar to the transmitted image in (a), thus presenting a clear communication performance improvement driven by the use of physical channel modeling coupled with model-based inversion.
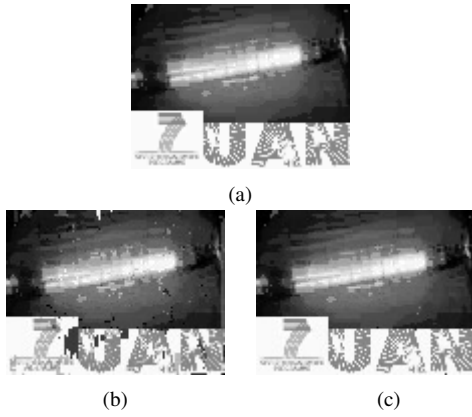
Fig. 8. Transmitted low resolution image (*a*), recovered image with PC estimation (*b*) and recovered image after processed by EPTR inversion (*c*).

IV. CONCLUSION

This paper presents a channel compensation method that uses environmental-based acoustic inversion designed for underwater communications. The Environmental-based Passive Time Reversal explores the influence of acoustic propagation physical parameters in benefit of equalization. CIR modeling from "a posteriori" acoustic propagation physical parameters which are reached by power optimization over a search space of "a priori" parameters relative to observed data estimated by PC or RegL1 are employed into passive time reversal. After conjugate reverse filtering, time compression/dilation compensation and phase recovery the original message is reconstructed. To the authors knowledge, this is the first time that a modeled CIR is successfully used to process real data in underwater communications. Experimental results are consistent and yield reasonably low mean square error, allowing to recover the transmitted image with low error, reaching MSE of approximately $-12\ dB$ over a real channel of $890\ m$ range and depth between $34\ m$ and $98\ m$. As future work, the authors intend to perform (i) time robustness tests of the UAN11 experiment data for the EPTR and the RegL1-based PTR, (ii) space robustness tests with different environments and (iii) optimization processing of the $\ell1$-norm regularization factor.

REFERENCES

[1] J. Gomes, A. Silva, and S. Jesus, "Adaptive spatial combining for passive time-reversed communications," *Journal of Acoustical Society of America*, pp. 1038–1053, August 2008.

[2] H. Song, "Time reversal communications with a mobile source," *Journal of Acoustical Society of America*, vol. 4, pp. 2623–26, Oct. 2013.

[3] R. G. Baraniuk, "Compressive sensing," *IEEE Signal Processing Magazine*, pp. 119–124, July 2007.

[4] E. Candes and J. Romberg, "Sparsity and incoherence in compressive sampling," *Inverse Problems I.O.P. Publishing*, pp. 969–985, July 2007.

[5] A. Parvulescu, "Signal Detection in a Multipath Medium by M.E.S.S. Processing," *Journal of Acoustical Society of America*, vol. 33, p. 1674, 1961.

[6] E. Shang, "Source depth estimation in waveguides," *Journal of Acoustical Society of America*, vol. 77, pp. 1413–1418, 1985.

[7] T. C. Yang, "A method of range and depth estimation by modal decomposition," *Journal of Acoustical Society of America*, vol. 83, pp. 1736–1745, 1988.

[8] M. Porter and A. Tolstoy, "The Matched Field Processing Benchmark Problems," *Journal of Computational Acoustics*, vol. 2, no. 3, pp. 161–184, 1994.

[9] A. Baggeroer, W. Kuperman, and H. Schmidt, "Matched-field processing: source localization in correlated noise as an optimum parameter estimation problem," *Journal of Acoustical Society of America*, vol. 83, pp. 571–587, 1988.

[10] C. Clay, "Optimum time domain signal transmission and source location in a waveguide," *Journal of Acoustical Society of America*, 1987.

[11] A. Tolstoy, O. Diachok, and L. Frazer, "Acoustic tomography via matched-field processing," *Journal of Acoustical Society of America*, vol. 89, pp. 1119–1127, 1991.

[12] M. D. Collins and W. A. Kuperman, "Focalization: environmental focusing and source localization," *Journal of Acoustical Society of America*, vol. 90, pp. 1410–1422, September 1991.

[13] S. Jesus, "Broadband matched-field processing of transient signals in shallow water," *Journal of Acoustical Society of America*, 1993.

[14] A. B. Baggeroer, W. A. Kuperman, and P. N. Mikhalevsky, "An overview of matched field methods in ocean acoustics," *IEEE Journal of Oceanic Engineering*, vol. 18, pp. 401–424, October 1993.

[15] M. B. Porter, *The BELLHOP Manual and User's Guide*. Heat, Light, and Sound Research, Inc., La Jolla, CA, USA, January 2011.

[16] H. C. Song, W. S. Hodgkiss, W. A. Kuperman, M. Stevenson, and T. Akal, "Improvement of time-reversal communications using adaptive channel equalizers," *IEEE Journal of Oceanic Engineering*, no. 31, pp. 487–96, 2006.

[17] M. Stojanovic, "Retrofocusing techniques for high rate acoustic communications," *Journal of Acoustical Society of America*, vol. 117, no. 3, pp. 1183–1185, 2005.

[18] M. Grant and S. Boyd, "Graph implementations for nonsmooth convex programs," in *Recent Advances in Learning and Control* (V. Blondel, S. Boyd, and H. Kimura, eds.), Lecture Notes in Control and Information Sciences, pp. 95–110, Springer-Verlag Limited, 2008.

[19] A. Tolstoy, *Matched Field Processing for Underwater Acoustics*. Singapore: World Scientific, 1993.

[20] E.J. Sullivan and Z.H. Michalopoulou and C. Yardim, "Model-based ocean acoustic signal processing", *Acoustics Today*, vol. 7, no. 3, pp. 8-15, 2011

[21] T. Husoy, M. Pettersen, B. Nilsson, T. Oberg, N. Warakagoda, and A. AbdiLie, "Implementation of an underwater acoustic modem with network capability," in *IEEE Oceans Conference*, (Spain), April 2011.

[22] A. Caiti, K. Grythe, J. M. Hovem, S. M. Jesus, A. Lie, A. Munafò, T. A. Reinen, A. Silva, and F. Zabel, "Linking Acoustic Communications and Network Performance: Integration and Experimentation of an Underwater Acoustic Network," *IEEE Journal of Oceanic Engineering*, vol. 38, pp. 758–771, October 2013.

[23] C. Soares, S. M. Jesus, and E. Coelho, "Environmental inversion using high-resolution matched-field processing," *Journal of Acoustical Society of America*, vol. 122, no. 6, pp. 3391–3404, 2007.

[24] F. Hlawatsch and G. Matz, *Wireless Communications Over Rapidly Time-Varying Channels*. Elsevier, 2011.